Chemistry & Biology
Brief Communication

Docking Motif-Guided Mapping of the Interactome of Protein Phosphatase-1

Annick Hendrickx,[1,2] Monique Beullens,[1,2,*] Hugo Ceulemans,[1,2] Tom Den Abt,[1] Aleyde Van Eynde,[1] Emilia Nicolaescu,[1] Bart Lesage,[1] and Mathieu Bollen[1]
[1]Laboratory of Biosignaling and Therapeutics, Department of Molecular Cell Biology, Faculty of Medicine, Katholieke Universiteit Leuven, B-3000 Leuven, Belgium
[2]These authors contributed equally to this work
*Correspondence: Monique.Beullens@med.kuleuven.be
DOI 10.1016/j.chembiol.2009.02.012

SUMMARY

The ubiquitous protein Ser/Thr phosphatase-1 (PP1) interacts with dozens of regulatory proteins that are structurally unrelated. However, most of them share a short, degenerate "RVxF"-type docking motif. Using a broad in silico screening based on a stringent definition of the RVxF motif, in combination with a multistep biochemical validation procedure, we have identified 78 novel mammalian PP1 interactors. A global analysis of the validated RVxF-based PP1 interactome not only provided insights into the conserved features of the RVxF motif but also led to the discovery of additional common PP1 binding elements, described as the "SILK" and "MyPhoNE" motifs. In addition to the doubling of the known mammalian PP1 interactome, our data contribute to the design of PP1 interaction networks. Notably, an interaction network linking PP1 interactors discloses a pleiotropic role of PP1 in cell polarity.

INTRODUCTION

Several thousands of human proteins have already been found to be phosphorylated in vivo (Olsen et al., 2006), mostly on serines or threonines. More than 400 human genes encode protein Ser/Thr kinases (Manning et al., 2002), but there are only about 40 genes that encode protein Ser/Thr phosphatases (Moorhead et al., 2007). This striking imbalance in gene number can be explained by a different diversification strategy during evolution. Indeed, protein kinases have mainly diversified by gene duplication and subsequent specification, whereas protein Ser/Thr phosphatases have diversified much more by increasing the variety of their regulatory subunits. At the holoenzyme level protein Ser/Thr kinases and phosphatases are equally diverse and show a similarly restricted substrate specificity. This is strikingly illustrated by protein phosphatase-1 (PP1), a ubiquitous and conserved enzyme that is estimated to catalyze about a third of all protein dephosphorylations in eukaryotic cells (Cohen, 2002; Ceulemans and Bollen, 2004; Moorhead et al., 2007). The mammalian PP1 isoforms, encoded by three genes, do not exist freely in the cell but tightly associate with a host of different proteins that determine when and where the phosphatase acts. PP1 interactors function as activity regulators, substrate-targeting proteins, substrate specifiers, and/or substrates. About 100 mammalian PP1 interactors have already been described and the rate of discovery of novel interactors shows as of yet no sign of abating, suggesting that many more interactors remain to be identified.

Using standard sequence analysis, PP1 interacting proteins do not show an obvious structural similarity because most of the few known PP1 docking motifs are short and degenerate (Terrak et al., 2004; Hurley et al., 2007) and flanked by unconserved stretches. A majority of the known PP1 interactors contain a variant of a motif that is now commonly referred to as the RVxF motif (Egloff et al., 1997; Ceulemans and Bollen, 2004). Crystallographic studies revealed that the RVxF motif binds as an extended β strand to a hydrophobic groove of PP1 that is 20 Å away from the catalytic site (Egloff et al., 1997; Terrak et al., 2004). Docking of the RVxF motif per se does not have a major effect on the conformation of the catalytic subunit but increases the local concentration of the interactor and thereby promotes secondary interactions that can affect the activity or substrate specificity of the phosphatase. Largely based on the conservation of established PP1-interacting RVxF motifs, Wakula et al. (2003) defined the RVxF motif as a five-residue motif with the consensus sequence [RK]-X(0,1)-[VI]-{P}-[FW], where X is any residue and {P} any residue but P. This definition is sensitive in that it covers about 90% of all known PP1-binding RVxF variants but lacks specificity because it occurs randomly in about a quarter of all proteins (Ceulemans and Bollen, 2006). More recently, Meiselbach et al. (2006) used site-directed mutagenesis to map the residues that are tolerated at each position of the RVxF motif and proposed the consensus sequence [HKR]-[ACHKMNQRSTV]-V-[CHKNQRST]-[FW]. The latter definition has only a sensitivity of about 40% but displays a 10-fold higher specificity than the Wakula definition (Ceulemans and Bollen, 2006).

Most PP1 interactors have been identified by classical biochemical approaches and two-hybrid screens. We have combined the specific Meiselbach definition and the sensitive Wakula definition of the PP1-interacting RVxF motif, as well as additional context filters, in an in silico search for novel PP1 interactors. This has led to the identification of 115 novel candidate PP1 interactors, 78 of which could be validated using independent biochemical approaches. Our study illustrates the feasibility of a bioinformatics-assisted, proteome-wide screening for structurally unrelated proteins that share a short, degenerate motif.

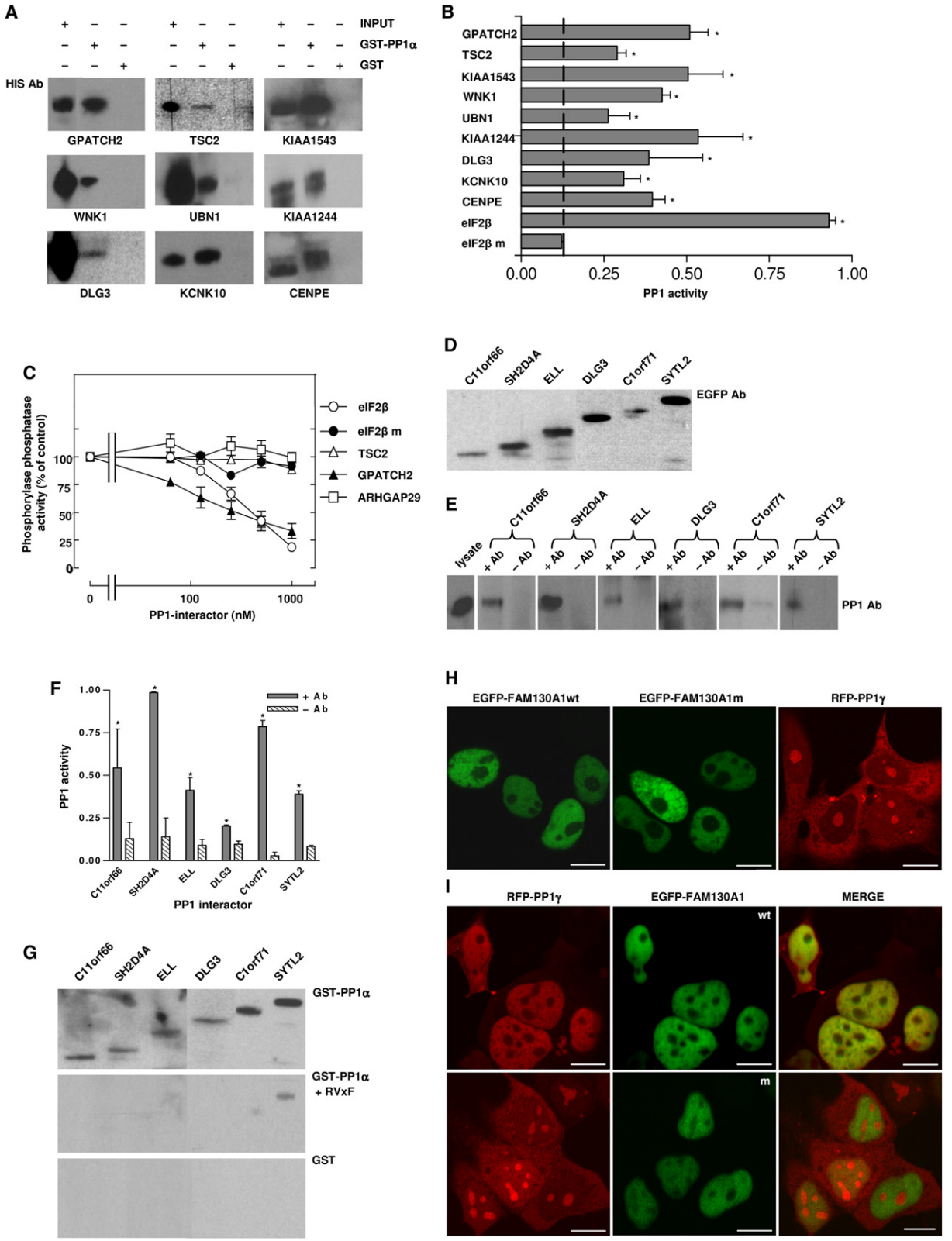

Figure 1. Biochemical Validation of the Interaction of Proteins with PP1

(A) Affinity-purified His-tagged fragments of the indicated proteins were used for pull-down experiments with GST-PP1α and GST. The His-tagged fragments in the mixture (input) and the precipitates were visualized by immunoblotting with anti-His antibodies. The figure shows representative data for proteins that were validated as PP1 interactors.

RESULTS AND DISCUSSION

In Silico Screening for Novel PP1 Interactors

The screening was performed on 14,725 sets of orthologous human, mouse, and rat protein sequences, obtained by an all-against-all BLASTP analysis. Because multiple sets can derive from a single gene, these 14,725 sets correspond to just over 14,000 genes or about two thirds of the protein encoding genome. Out of the 14,725 orthologous sets, 397 contained an RVxF variant that was conserved in all three species and compatible with both the sensitive Wakula definition and the specific Meiselbach definition (Wakula et al., 2003; Meiselbach et al., 2006). This screening thus excluded proteins, such as Inhibitor-2, that have a RVxF motif that does not conform to both definitions. The list of predicted PP1 interactors was further reduced using additional filters. First, since the RVxF motif is known to be present in a flexible loop that adopts a β strand conformation upon binding to PP1 (Egloff et al., 1997), proteins with an RVxF variant in a globular domain were removed from the list. Second, since PP1 only exists intracellularly, proteins with a consensus RVxF motif in an extracellular or transmembrane domain were considered to be false positives. Third, 22 sets represented already known PP1 interactors and they were not further analyzed. Altogether, these additional filters reduced the number of novel candidate interactors of PP1 to 115 (see Table S1 available online).

Validation of the Interaction with PP1

To biochemically validate the interaction with PP1, we first expressed fragments of the putative interactors as His-tagged fusion proteins in bacteria and affinity purified the fusions on Ni^{2+}-Sepharose. The fragments were about 200 residues on average with the RVxF motif in the middle, as detailed in Table S1. This expression and purification approach succeeded for 103 out of the 115 predicted interactors. The purified proteins were tested for their ability to bind PP1 in pull-down assays with glutathione S-transferase (GST)-tagged PP1α (Figures 1A and 2). GST served as a negative control. Conversely, the His-tagged fusions, bound to Ni^{2+}-Sepharose, were incubated with the purified catalytic subunit of PP1 and the retained phosphatase activity was quantified with glycogen phosphorylase *a* as substrate, after prior trypsinolysis to release the fully active catalytic subunit (Figures 1B and 2). In the latter assays, the established PP1 interactor His-eIF2β was used as a positive control and His-eIF2β with a mutated RVxF motif as a negative control (Wakula et al., 2006). Both tests yielded essentially the same results and validated 78 out of the 103 tested proteins as in vitro interactors of PP1. Because many PP1 interactors are inhibitory with exogenous substrates (Bollen, 2001), we also examined the effect of the novel interactors on the phosphorylase phosphatase activity of PP1. More than half of these proteins (i.e., 49 out of 78) were inhibitory (Figures 1C and 2), which represents additional and independent biochemical evidence for their interaction with PP1 and is suggestive for their role as activity regulators or substrate specifiers. However, because the effects of PP1 interactors are substrate dependent, their exact function can only be explored once the substrates of the corresponding holoenzymes are known. The biochemical validation tests shown in Figures 1A–1C were also used for five previously established PP1 interactors and five randomly chosen proteins (Figure S1). In these tests, the first five proteins were confirmed as PP1 interactors while the randomly chosen proteins were all negative, attesting to the specificity and sensitivity of the adopted assays. It is also worthy of note that 16 paralogs of the 78 novel and validated human PP1 interactors also had an RVxF(-like) motif at the same position (Table S2). Although these paralogs were not retained during the initial in silico screening with the adopted filters they are also possible PP1 interactors.

It could be argued that the detected in vitro interaction with PP1 (Figures 1A–1C and 2) is artifactual and results from the use of protein fragments. Therefore, we expressed 21 of the validated PP1 interactors as full-length proteins with an N-terminal enhanced green fluorescent protein (EGFP) tag in HEK293 cells and immunoprecipitated the fusion proteins with anti-EGFP antibodies (Figure 1D and data not shown). Of the 21 examined proteins, 17 coimmunoprecipitated with endogenous PP1, as detected by immunoblotting with PP1 antibodies (Figures 1E and 2) and by the assay of trypsin-revealed phosphorylase phosphatase activity (Figures 1F and 2). The immunoprecipitated interactors were also used for overlay assays with purified GST-PP1α after SDS-PAGE (Figures 1G and 2). In the latter assays, 18 out of the 21 tested proteins bound GST-PP1α, but not GST. Importantly, GST-PP1α was not retained when saturated with a synthetic RVxF peptide, indicating that the binding to the interactors was specific and depended on an accessible RVxF-binding channel. Collectively, these experiments with full-length proteins largely confirmed the data obtained with

(B) The His-tagged interactor fragments, bound to Ni^{2+}-Sepharose, were incubated with purified PP1. The retained PP1 was quantified by the assay of the trypsin-revealed phosphorylase phosphatase activity. eIF2β served as a positive control and eIF2β with a mutated RVxF motif (eIF2βm) as a negative control. The phosphatase activities (bars) are expressed as means ± SEM (n = 3). *$p < 0.05$, as compared to the value with eIF2βm (paired t test).

(C) Effects of the indicated affinity-purified interactor fragments on the phosphorylase phosphatase activity of purified PP1. The activities are expressed as means ± SEM (n = 3).

(D) The indicated proteins were expressed as EGFP-tagged fusions in HEK293 cells and immunoprecipitated with anti-EGFP antibodies, as verified by immunoblotting.

(E) The coimmunoprecipitated endogenous PP1 was detected by immunoblotting with anti-PP1 antibodies.

(F) The coimmunoprecipitated PP1 was also quantified (gray bars) by the assay of the trypsin-revealed phosphorylase phosphatase activity (means ± SEM; n = 3). *$p < 0.05$ (paired t test), as compared to the value without primary antibodies (hatched bars).

(G) In addition, the immunoprecipitated proteins were processed for SDS-PAGE, blotted, and incubated with GST-PP1α, GST-PP1α that was saturated with a synthetic RVxF peptide, or GST. The retained GST (fusion) was visualized with anti-GST antibodies.

(H) Subcellular localization of transiently expressed EGFP-Fam130A1, EGFP-Fam130A1 with a mutated RVxF motif (EGFP-Fam130A1m), and RFP-PP1γ in HEK293 cells, as detected by fluorescence microscopy.

(I) EGFP-Fam130A1wt (top) or EGFP-Fam130A1m (bottom) were coexpressed with RFP-tagged PP1γ. The figure shows the subcellular localization of RFP-PP1γ (left), EGFP-Fam130A1wt and m(utant) (middle), and the merged pictures (right). Size bar: 10 μm.

A

Gene symbol	Inhibition of PP1	Co-IP of PP1	Overlay with PP1	Gene symbol	Inhibition of PP1	Co-IP of PP1	Overlay with PP1
C1orf71	+	+	+	LRRC68	+		
C7orf47	+			MAP1B	–		
C11orf66	–	+	+	MCM7	–		
C14orf50	+			MKI67	+		
CASC1	–			MPHOSPH10	+	–	–
CASC5	+			MYO1D	+		
CCDC8	+			ORC5L	–		
CCDC128	–			PCDH11X	+		
CD2BP2	+			PCIF1	+		
CENPE	–			PHRF1	–		
CEP192	+	+	+	PKMYT1	+		
CHCHD3	–	+	+	PMP22CD	+		
CHCHD6	–			RBM26	+		
CSMD1	–			RIMBP2	+		
DDX31	–			RPGRIP1L	–		
DEPDC2	–			RRP1B	+		
DLG2	+			SACS	–		
DLG3	+	+	+	SFI1	+	+	+
DYSFIP1	+	+	+	SH2D4A	+	+	+
DZIP3	–	+	–	SH3RF2	+	+	+
ELFN1	+			SLC7A14	+		
ELFN2	+			SPATA2	–		
ELL	+	+	+	SPOCD1	+		
FAM130A1	+	+	+	SPRED1	+	+	+
FAM130A2	+			SYTL2	+	+	+
FARP1	+			TMEM132C	+		
FKBP15	+	–	–	TMEM132D	+	–	+
GPATCH2	+			TRIM42	–		
GPR12	–			TRPC4AP	–	+	+
GRXCR1	+			TSC2	–	+	+
HYDIN	–			TSKS	+		
ITPR3	–			UBN1	–		
JARID1B	–			VPS54	–		
KCNK10	–			WDR81	+		
KIAA0430	+			WNK1	+	+	+
KIAA0649	+			ZBTB38	–		
KIAA1244	+			ZCCHC9	+		
KIAA1543	+			ZFYVE1	+	–	+
LMTK3	+			ZSWIM3	–		

B

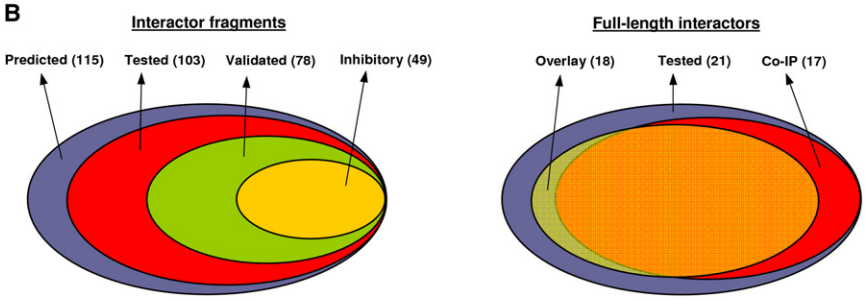

Figure 2. Novel Interactors of PP1

(A) All listed genes encode proteins that interact with PP1, as tested with His-tagged fragments in GST pull-down experiments (see Figure 1A) and PP1 retention assays on Ni^{2+}-Sepharose (see Figure 1B). A subset of the interactors were also expressed as EGFP-tagged full-length proteins and tested for their ability to coimmunoprecipitate endogenous PP1 (see Figures 1E and 1F) and to bind PP1 in overlay assays (see Figure 1G).

(B) The left diagram illustrates the extent to which the predicted PP1 interactors were validated using biochemical assays with interactor fragments. Predicted interactors (115), tested interactors (103), interactors validated with GST-PP1α pull-down assays and PP1 retention assays on Ni^{2+}-Sepharose (78), and fragments that were inhibitory to PP1, using glycogen phosphorylase as a substrate (49). The diagram at the right compares the validation results for full-length interactors following their transient expression in HEK293 cells. Tested proteins (21), coimmunoprecipitation with endogenous PP1 (17), and overlay with GST-PP1 (18).

the interactor fragments (see Figure 2 for a detailed comparison of all validation tests). That not all full-length proteins could be shown to interact with PP1 is not surprising since this interaction can be cell type and context dependent (Bollen, 2001; Ceulemans and Bollen, 2004).

When overexpressed, some PP1 interactors cause a subcellular redistribution of endogenous PP1 (Lesage et al., 2004). We have used this in situ test of PP1 interaction for two of the newly identified PP1 interactors, namely Fam130A1 (Figures 1H and 1I) and ELL (Figure S2). Fam130A1 displayed a uniform nuclear distribution but was excluded from the nucleoli, while ELL showed a speckled nuclear distribution, consistent with its described association with the Cajal bodies (Polak et al., 2003). The expression of EGFP-tagged fusions of Fam130A1 or ELL caused a subnuclear redistribution of coexpressed red fluorescent protein (RFP)-tagged PP1γ in that it lost its characteristic nucleolar enrichment and colocalized with the EGFP fusions. This altered distribution of RFP-PP1γ was not seen following the expression of Fam130A1 or ELL with a mutated RVxF motif (V and F to A), attesting to the importance of this PP1 docking motif for the redistribution of PP1γ.

The Identification of Additional Common PP1 Interaction Motifs

Currently, we know of 143 mammalian genes encoding PP1 interactors with a validated RVxF motif. These comprise 65 previously described PP1 interactors (Table S3) and the 78 novel interactors listed in Figure 2A. We have used this expanded PP1 interactome to reevaluate the conserved features of the RVxF motif and its flanking residues (Table S4). Consistent with a previous proposal (Egloff et al., 1997; Wakula et al., 2003), the RVxF motif is actually a 5 residue motif. It has the sequence $[K_{55}R_{34}][K_{28}R_{26}][V_{94}I_6]\{FIMYDP\}[F_{83}W_{17}]$ (see Table S4 for a more detailed definition), where the numbers in subscript refer to the percentages of residue occurrence and braced residues are excluded. The most conserved residues are those at positions 1, 3, and 5. Interestingly, while some residues (FIMYDP) never occur at position 4, this position is clearly enriched for R (17%), K (11%), S (21%), and T (18%). The enrichment for S and T probably serves a regulatory function as phosphorylation at this position is known to disrupt the binding of PP1 (Egloff et al., 1997). Another striking feature is the overrepresentation of basic and acidic residues at N-terminal and C-terminal positions to the RVxF motif, respectively.

Since PP1 interactor complexes often have multiple binding sites, we have subsequently examined whether the RVxF-based

Table 1. Additional Common PP1 Binding Motifs in Interactors with a Validated RVxF Motif

Gene Name	MyPhoNE		RVxF
myo16	^{24}RCEQIKAY	(22)	PKVHF^{58}
ppp1r12a	^{10}RNEQLKRW	(16)	TKVKF^{38}
ppp1r12b	^{19}RAEQLRRW	(25)	PRVRF^{56}
ppp1r16a	^{30}RAQQVKMW	(27)	KQVLF^{69}
ppp1r16b	^{30}RAQQLKKW	(24)	KKVSF^{66}
sh2d4a	^{32}REEQIRRW	(24)	KSVHW^{68}
sh2d4b	^{32}REEQLRRW	(26)	KHIQW^{70}
Gene Name	SILK		RVxF
casc5	^{25}SILK	(28)	RRVSF^{61}
c1orf71	^{621}SILK	(19)	RRVRF^{648}
fam130a1	^{53}SILK	(7)	KNVRF^{68}
fam130a2	^{52}SILK	(7)	KNVHF^{67}
ppp1r2	^{13}GILK	(26)	KSQKW^{47}
sytl2	^{271}GILK	(55)	KHVRF^{334}
wbp11	^{165}SILK	(48)	RKVGF^{221}

The superscript numbers refer to the position of the residue. The numbers in parentheses represent the number of residues between the two PP1 binding motifs.

PP1 interactome also shares other well-defined PP1 binding elements. The myosin phosphatase targeting subunit Mypt1, encoded by *ppp1r12a*, has an N-terminal PP1 interaction motif with the consensus sequence RxxQ[VIL][KR]x[YW] that is involved in substrate recognition (Terrak et al., 2004). Interestingly, this motif, coined the myosin phosphatase N-terminal element or "MyPhoNE," is also present in six other PP1 interactors, always N-terminal to the RVxF motif (Table 1).

One of the PP1 docking motifs of Inhibitor-2 conforms to the consensus sequence [GS]IL[RK] (Huang et al., 1999; Wakula et al., 2003; Hurley et al., 2007) and is here referred to as the "SILK" motif. The SILK motif is essential for potent inhibition by Inhibitor-2 (Huang et al., 1999; Connor et al., 2000) and can functionally replace the RVxF motif in NIPP1 (Wakula et al., 2003). We found that the SILK motif also occurs in six other PP1 interactors and is always N-terminal to the RVxF motif (Table 1). To delineate the relative importance of the SILK and RVxF motifs for PP1 binding we mutated these motifs, either alone or combined, in SIPP1 and Fam130A1, and examined the effect of these mutations on the binding of PP1 (Figure S3). For SIPP1, mutation of either the SILK or the RVxF motif already drastically reduced the interaction with PP1. In contrast, mutation of the SILK motif in Fam130A1 only had a measurable effect on PP1 binding when combined with a mutation of the RVxF motif. These data suggest that the importance of the SILK motif for the anchoring of PP1 is interactor dependent.

The Design of PP1 Interaction Networks

The identification of 78 novel PP1 interactors, which roughly represents a doubling of the known mammalian PP1 interactome, facilitates the literature-assisted design of PP1 networks and yields new insights into the functional diversity of PP1. This is illustrated in Figure 3 for a "cell polarity" network, which comprises seven previously identified and nine novel PP1 interactors. This network shows how the PP1 interactome is connected to signaling by the GTPases Cdc42, Rac, and Rho. It suggests that PP1 sides consistently with Cdc42 and Rac, in opposition of a cascade of protein kinases allied with Rho. PP1 thereby supports cell growth, cellular protrusions and adhesions, and the response to hypotonicity. The observed alliance of PP1 with Cdc42 and Rac offers a biological framework for the generation of functional hypotheses about novel PP1 interactors. For example, like the PP1-binding kinetochore protein Casc5, Cdc42 has been implicated in the capture of microtubules at the kinetochore (Yasuda et al., 2004). PP1 recruitment to centrosomal proteins like Nek2A (Mi et al., 2007) or the PP1 interactors Sfi1 and Cep192 (this work) may hint at additional functions of PP1 in microtubule organization. The interaction of PP1 with Vps54 or the synaptotagmin-like protein Sytl2 may fit in nicely with the established role of Cdc42 in exo- and endocytosis (Yu and Bement, 2007). In yeast, Arf1 and Arf2 and the related protein Bni4 recruit PP1 to the Cdc42-orchestrated septin ring at the bud neck and the base of mating protrusions, respectively (Larson et al., 2008). The related vertebrate Phactrs also bind PP1 and may hence target PP1 to the incipient cytokinetic cleavage furrow. In many of these cases, a placement of novel PP1 interactors in the Cdc42 framework will add tentative direction to the functional effects of the interaction.

SIGNIFICANCE

The bioinformatics-assisted screening tools that we have used to search for PP1 interactors can be easily adapted to identify any group of proteins that share a short, degenerate binding motif. Examples include substrates of calcineurin with the PxIxIT-type docking motif (Roy et al., 2007) and proteins with the RFxV-type kinase docking motif (Vitari et al., 2006). However, the biochemical validation of the predicted interactions is equally important and the procedures that we have used can not necessarily be applied to other groups of proteins. For example, we have extensively made use of interactor fragments that were delineated rather arbitrarily, without taking into consideration the protein domain structure. This approach clearly did not hamper PP1 interaction, probably because the RVxF motif, and possibly also other PP1 binding domains, show little 3D structure in their unbound form (Dancheck et al., 2008), but may be problematic when used for the validation of other protein-protein interactions.

EXPERIMENTAL PROCEDURES

In Silico Analysis

As a source of maximally comprehensive yet minimally redundant sequence sets for human, mouse, and rat proteins, we downloaded for each of these species set 3.13 of the International Protein Index (ftp://ftp.ebi.ac.uk/pub/databases/IPI/). The 57,032 human, 50,489 mouse, and 39,474 rat sequences were compared in all-against-all BLASTP searches, using a Perl script with the database size parameter (−z) set to 100,000,000, the low-complexity filtering flag (−F) switched on, and otherwise default parameters. A second Perl script assembled the 14,725 orthologous sets of reciprocal best BLASTP hits among the three studied species and filtered them for the presence in all three sequences of at least one instance that fitted with both the Wakula and Meiselbach definition of the RVxF-type PP1 docking motif (Wakula et al., 2003; Meiselbach et al., 2006).

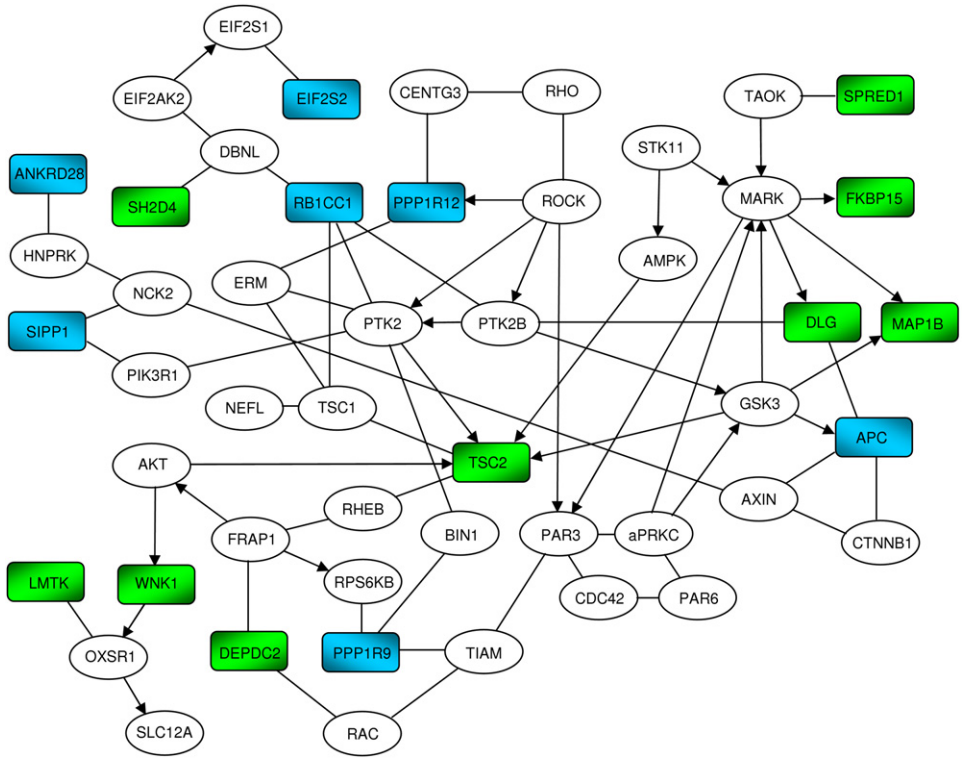

Figure 3. An Interaction Network that Links PP1 to Cell Polarity
The network was composed based on published data, with previously described (blue rectangles) and novel (green rectangles) interactors of PP1. The arrows indicate known kinase substrates.

Biochemical Validation of the Interaction with PP1

The bacterially expressed polyhistidine-tagged interactor fragments (Supplemental Experimental Procedures and Tables S1 and S5) were used for pull-down experiments with Ni^{2+}-Sepharose and as inhibitors of the phosphorylase phosphatase activity of PP1 (Wakula et al., 2006). The catalytic subunit of PP1 was purified from rabbit skeletal muscle and is a mixture of all three isoforms (DeGuzman and Lee, 1988). For the GST pull-down assays, equimolar amounts of GST and GST-PP1α were preincubated for 1 hr at 10°C with glutathione agarose. These precoupled GST and GST-PP1α matrices were incubated with the His fragments for 1 hr. The precipitates were analyzed by immunoblotting with anti-His antibodies. For the overlay with GST-PP1α, the immunoprecipitated proteins were processed for SDS-PAGE and blotted on polyvinylidene fluoride membranes. The blot was blocked with BSA and incubated overnight with GST-PP1α, GST-PP1α saturated with 100 μM of the synthetic RVxF peptide NIPP1 (197–206), or GST alone. Finally, the bound PP1 was visualized using anti-GST antibodies. HEK293T cells were cultured and transfected as described previously (Lesage et al., 2004).

SUPPLEMENTAL DATA

Supplemental Data include Supplemental Experimental Procedures, three figures, and five tables and can be found with this article online at http://www.cell.com/chemistry-biology/supplemental/S1074-5521(09)00079-9.

ACKNOWLEDGMENTS

This research was funded by a PhD grant of the Institute for the Promotion of Innovation through Science and Technology in Flanders (IWT-Vlaanderen) to Annick Hendrickx. Nicole Sente, Fabienne Withof, and Annemie Hoogmartens provided expert technical assistance. This work was financially supported by the Fund for Scientific Research-Flanders (grant G.0487.08), a Flemish Concerted Research Action, and the Prime Minister's office (IAP/6-28). Additional acknowledgements are in the Supplemental Experimental Procedures.

Received: November 25, 2008
Revised: February 25, 2009
Accepted: February 25, 2009
Published: April 23, 2009

REFERENCES

Bollen, M. (2001). Combinatorial control of protein phosphatase-1. Trends Biochem. Sci. *26*, 426–431.

Ceulemans, H., and Bollen, M. (2004). Functional diversity of protein phosphatase-1, a cellular economizer and reset button. Physiol. Rev. *84*, 1–39.

Ceulemans, H., and Bollen, M. (2006). A tighter RVxF motif makes a finer Sift. Chem. Biol. *13*, 6–8.

Cohen, P.T. (2002). Protein phosphatase 1—targeted in many directions. J. Cell Sci. *115*, 241–256.

Connor, J.H., Frederick, D., Huang, H., Yang, J., Helps, N.R., Cohen, P.T., Nairn, A.C., DePaoli-Roach, A., Tatchell, K., and Shenolikar, S. (2000). Cellular mechanisms regulating protein phosphatase-1. A key functional interaction between inhibitor-2 and the type 1 protein phosphatase catalytic subunit. J. Biol. Chem. *275*, 18670–18675.

Dancheck, B., Nairn, A.C., and Peti, W. (2008). Detailed structural characterization of unbound protein phosphatase 1 inhibitors. Biochemistry *47*, 12346–12356.

DeGuzman, A., and Lee, E.Y.C. (1988). Preparation of low-molecular-weight forms of rabbit skeletal muscle protein phosphatases. Methods Enzymol. *159*, 356–368.

Egloff, M.P., Johnson, D.F., Moorhead, G., Cohen, P.T., Cohen, P., and Barford, D. (1997). Structural basis for the recognition of regulatory subunits by the catalytic subunit of protein phosphatase 1. EMBO J. *16*, 1876–1887.

Huang, H.B., Horiuchi, A., Watanabe, T., Shih, S.R., Tsay, H.J., Li, H.C., Greengard, P., and Nairn, A.C. (1999). Characterization of the inhibition of protein phosphatase-1 by DARPP-32 and inhibitor-2. J. Biol. Chem. *274*, 7870–7878.

Hurley, T.D., Yang, J., Zhang, L., Goodwin, K.D., Zou, Q., Cortese, M., Dunker, A.K., and DePaoli-Roach, A.A. (2007). Structural basis for regulation of protein phosphatase 1 by inhibitor-2. J. Biol. Chem. *282*, 28874–28883.

Larson, J.R., Bharucha, J.P., Ceaser, S., Salamon, J., Richardson, C.J., Rivera, S.M., and Tatchell, K. (2008). Protein phosphatase type 1 directs chitin synthesis at the bud neck in *Saccharomyces cerevisiae*. Mol. Biol. Cell *19*, 3040–3051.

Lesage, B., Beullens, M., Nuytten, M., Van Eynde, A., Keppens, S., Himpens, B., and Bollen, M. (2004). Interactor-mediated nuclear translocation and retention of protein phosphatase-1. J. Biol. Chem. *279*, 55978–55984.

Manning, G., Whyte, D.B., Martinez, R., Hunter, T., and Sudarsanam, S. (2002). The protein kinase complement of the human genome. Science *298*, 1912–1934.

Meiselbach, H., Sticht, H., and Enz, R. (2006). Structural analysis of the protein phosphatase 1 docking motif: molecular description of binding specificities identifies interacting proteins. Chem. Biol. *13*, 49–59.

Mi, J., Guo, C., Brautigan, D.L., and Larner, J.M. (2007). Protein phosphatase-1alpha regulates centrosome splitting through Nek2. Cancer Res. *67*, 1082–1089.

Moorhead, G.B., Trinkle-Mulcahy, L., and Ulke-Lemée, A. (2007). Emerging roles of nuclear protein phosphatases. Nat. Rev. Mol. Cell Biol. *8*, 234–244.

Olsen, J.V., Blagoev, B., Gnad, F., Macek, B., Kumar, C., Mortensen, P., and Mann, M. (2006). Global, in vivo, and site-specific phosphorylation dynamics in signaling networks. Cell *127*, 635–648.

Polak, P.E., Simone, F., Kaberlein, J.J., Luo, R.T., and Thirman, M.J. (2003). ELL and EAF1 are Cajal body components that are disrupted in MLL-ELL leukemia. Mol. Biol. Cell *14*, 1517–1528.

Roy, J., Li, H., Hogan, P.G., and Cyert, M.S. (2007). A conserved docking site modulates substrate affinity for calcineurin, signaling output, and in vivo function. Mol. Cell *25*, 889–901.

Terrak, M., Kerff, F., Langsetmo, K., Tao, T., and Dominguez, R. (2004). Structural basis of protein phosphatase 1 regulation. Nature *429*, 780–784.

Vitari, A.C., Thastrup, J., Rafiqi, F.H., Deak, M., Morrice, N.A., Karlsson, H.K., and Alessi, D.R. (2006). Functional interactions of the SPAK/OSR1 kinases with their upstream activator WNK1 and downstream substrate NKCC1. Biochem. J. *397*, 223–231.

Wakula, P., Beullens, M., Ceulemans, H., Stalmans, W., and Bollen, M. (2003). Degeneracy and function of the ubiquitous RVXF motif that mediates binding to protein phosphatase-1. J. Biol. Chem. *278*, 18817–18823.

Wakula, P., Beullens, M., van Eynde, A., Ceulemans, H., Stalmans, W., and Bollen, M. (2006). The translation initiation factor eIF2beta is an interactor of protein phosphatase-1. Biochem. J. *400*, 377–383.

Yasuda, S., Oceguera-Yanez, F., Kato, T., Okamoto, M., Yonemura, S., Terada, Y., Ishizaki, T., and Narumiya, S. (2004). Cdc42 and mDia3 regulate microtubule attachment to kinetochores. Nature *428*, 767–771.

Yu, H.Y., and Bement, W.M. (2007). Control of local actin assembly by membrane fusion-dependent compartment mixing. Nat. Cell Biol. *9*, 149–159.